Research of Partial Discharge Localization Method in GIS Based on UHF Technique

JUNHUA LIU[1], MING YAO[2], CHENGJUN HUANG[1], LINPENG YAO[1],
HUI WANG[1], XIUCHEN JIANG[1]
[1]Department of Electrical Engineering, [2] Department of Production and Technology
[1]Shanghai Jiao Tong University, [2]Shanghai Municipal Electrical Power Company
[1]Shanghai, 200240, [2]Shanghai, 200122
CHINA.
drunhua@sjtu.edu.cn http://www.sjtu.edu.cn

Abstract: - Some small defects like fix protrusion or free moving particles exist in GIS can induce partial discharge (PD) which will deteriorate insulation condition and eventually cause insulation breakdown when GIS are in service. It is very important to detect and locate the PD signal for early detection of insulation defects and preventing insulation failure. Time of flight method which based on Ultra High Frequency (UHF) technique is widely used for locating PD in GIS for the merits such as simple principle and easy implementation. But in application, the time of flight method can hardly be applied effectively and will induce errors if the initial pulse of the PD signal is small and blurry or its signal-to-noise ratio (SNR) is too low. In this paper, the characteristics of electromagnetic wave (EM-wave) propagation route in GIS were investigated and a new localization method was proposed. The simulation and experiment results show that the EM-wave signals induced by PD in GIS are related with EM-wave propagation routes, which were decided by the location of PD source and detector's position. The experiment results show that the proposed PD localization method which based on the characteristics of EM-wave propagation route can locate the PD signal well and effectively in the case that the initial pulse of PD signals is very small and blurry when PD source locates near the outer conductor of GIS.

Key-Words: - GIS, partial discharge, UHF method, localization, EM-wave, propagation route

1 Introduction

In recent years, gas insulated switchgear (GIS) are widely used in power substations as the advantages of small volume, good reliability and long repair period. But in the process of manufacturing and assembling, some small defects like fix protrusion or free moving particles can be introduced in GIS for some technical reasons. The existence of small defects can induce partial discharge (PD) which will deteriorate insulation condition and eventually cause insulation breakdown when GIS are in service. Thus, the detection of PD is very important for early detection of insulation defects, preventing insulation failure and improving the power supply reliability [1-5]. Standardized method of PD detection defined by IEC 60270[6] is the best way used in the factory, but there are some limitations such as interference from electromagnetic noise is difficult to be discriminated and PD localization is not possible when it is used for on-site PD detection in GIS. To solve these problems, Ultra High Frequency (UHF) method has been introduced and widely used for on-site testing of GIS recently [7-12].

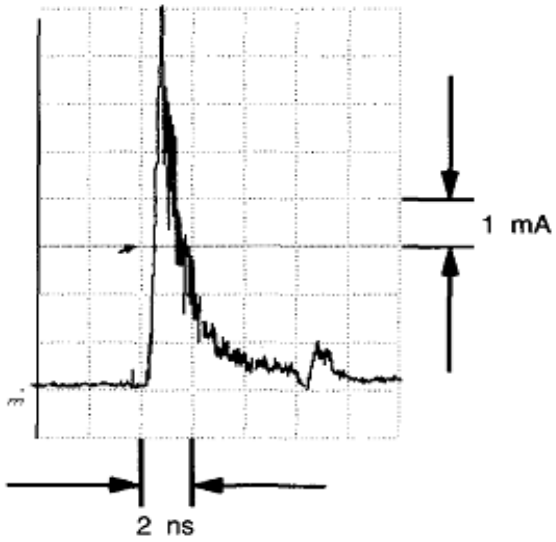

Fig.1 Typical partial discharge waveform

Partial discharge in SF6 generate a very short current pulse (Fig.1), which flowing at the defect of GIS is a very short burst with very short rise-time (< 1ns) [13]. The very fast rise-time of PD pulse excites electromagnetic wave (EM-wave) with frequency components as high as the order of GHz [14].UHF method based on detecting the UHF band (300MHz to 3GHz) electromagnetic wave signal emitted by the PD pulse is relatively free from external noises and has good sensitivity during on-site testing. The additional and valuable advantage of this technique is the capacity of locating PD source in GIS.

It's needed to locate the PD source for finding the insulation defect when PD happened in GIS. Time of flight method is widely used for locating PD in GIS for the merits such as simple principle, easy implementation and good veracity [15-17]. But if the initial pulse of the PD signal is small and blurry or its signal-to-noise ratio (SNR) is too low, the time of flight method can hardly be applied effectively and will induce errors. Inputting UHF signal by a monopole probe protruding through the outer conductor of GIS and detecting the signal by UHF coupler which mounted directly in line with the source probe, it was found that the initial pulse of signal was small and a much larger signal occurred a short time later which can be explained by the propagation of the normal electric field around the inner surface of the outer conductor [18]. Yet the phenomena and characteristic of EM-wave propagation route have not been researched thoroughly. Will the propagation route be affected by PD source position? What is the relationship between the signal waveform and UHF sensor position?

For improving the accuracy and validity of PD localization, the characteristics of EM-wave propagation route in GIS were investigated in this paper. The relationships between the EM-wave signals in GIS and the positions of PD source and detector were analyzed by constructing relatively simulation models and experiment system. As a result, a partial discharge localization method in time domain based on EM-wave propagation route was proposed which can locate the PD source well when the initial pulse of PD signal is small and blurry.

2 EM-waves in GIS

GIS can be regarded as a coaxial waveguide with the radius of inner conductor and outer conductor are *a* and *b*, as shown in Fig 2. It is known from EM- wave theory that not only TEM mode but also TE and TM modes can exist in coaxial waveguide. But TE and TM modes have cut-off frequencies and can only propagate at frequencies above their own cut-off frequency while TEM mode can propagate at any frequency.

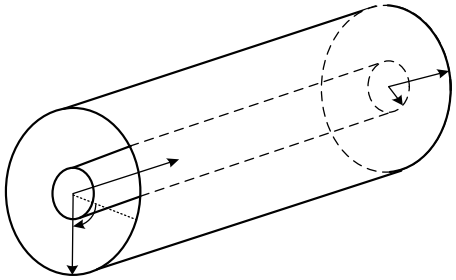

Fig.2 Coaxial wave-guide system

The electric field and magnetic field of EM-waves propagating in coaxial waveguide are satisfied with following Helmholtz equation [19]

$$\begin{cases} \nabla_t^2 \mathbf{E} + k_c^2 \mathbf{E} = 0 \\ \nabla_t^2 \mathbf{H} + k_c^2 \mathbf{H} = 0 \end{cases} \quad (1)$$

where $\mathbf{E}$ is the electric field vector. $\mathbf{H}$ is the magnetic field vector. ∇_t is the transverse Laplacian. $k_c^2 = k^2 + \gamma^2$ is the cut-off wave number. $\gamma = \alpha + j\beta$ is the propagation constant, while α is the attenuation constant and β is the phase-shift constant. $k = \omega\sqrt{\mu\varepsilon}$ is the EM-wave number, while *w* is the angular frequency, μ is the medium permeability and ε is the medium permittivity.

To reduce the complexity of the EM wave equation, the three classifications of EM wave propagating mode are considered separately. Beside the unique TEM mode, an infinite number of higher order modes exists which designated by subscripts as TE_{mn} and TM_{mn}. Accordingly, the expressions relating to these mode types contain summations over all *n* and *m*.

TEM mode (E_z=0, H_z=0) is the main mode in the coaxial waveguide. The electric field and magnetic field of TEM mode satisfied with following the Laplace equation

$$\begin{cases} \nabla_t^2 \mathbf{E} = 0 \\ \nabla_t^2 \mathbf{H} = 0 \end{cases} \quad (2)$$

According the boundary condition $r=a$, potential $\Phi=u_0$, and $r=b$, potential $\Phi=0$. The EM field propagating along *z* orientation can be expressed as

$$\begin{cases} E_r = \dfrac{u_0}{r\ln(b/a)} e^{-jkz} \\ H_\varphi = E_r / \eta \end{cases} \quad (3)$$

where E_r is the scalar weight in the radius orientation of the electric field vector **E**. $H\varphi$ is the scalar weight in the circle orientation of the magnetic field vector **H**. $\eta = \sqrt{\mu/\varepsilon}$ is wave impedance.

TM mode ($H_z = 0$, $E_z \neq 0$)

$$E_z = [B_1 J_m(k_c r) + B_2 N_m(k_c r)] C^{\cos m\varphi}_{\sin m\varphi} e^{-j\beta z} \quad (4)$$

where E_z is the scalar weight in the z orientation of the electric field vector **E**. $J_m(x)$ is the first kind, order m of Bessel function. $N_m(x)$ is the second kind, order m of Bessel function.

According the boundary condition $r=a$, $E_z=0$ and $r=b$, $E_z=0$. The equation (4) becomes

$$J_m(k_c a)N_m(k_c b) - J_m(k_c b)N_m(k_c a) = 0 \quad (5)$$

TE mode ($E_z = 0$ $H_z \neq 0$)

$$H_z = [C_1 J_m(k_c r) + C_2 N_m(k_c r)] D^{\cos m\varphi}_{\sin m\varphi} e^{-j\beta z} \quad (6)$$

where H_z is the scalar weight in the z orientation of the electric field vector **H**.

According the boundary condition $r=a$, $E_\varphi = 0$ and $r=b$, $E_\varphi = 0$. The equation (6) becomes

$$J_m'(k_c a)N_m'(k_c b) - J_m'(k_c b)N_m'(k_c a) = 0 \quad (7)$$

where $J_m'(x)$ is the first derivative of the Bessel function $J_m(x)$. $N_m'(x)$ is first derivative of the Bessel function $N_m(x)$.

The equation (5) and (7) are the eigenvalue equations of TM and TE modes, which can decide the cut-off wave number k_c. When the frequency of high order modes is high enough ($k>k_c$), β is a real number and the travelling wave factor is $e^{-j\beta z}$, EM-wave propagates along z axis. But when the frequency of high order modes is low ($k<k_c$), β is an imaginary number and the travelling wave factor $e^{-j\beta z}$ becomes an attenuation factor $e^{|\beta| z}$, EM-wave attenuates very fast along z axis and can't propagate in coaxial waveguide. When $k=k_c$, $\beta=0$, this is the dividing line between propagation and cut-off and it is called critical condition.

The cut-off frequency of high order mode can be approximately obtained by the following equation [20]

$$f_{cmn} = k_{cmn} / (2\pi\sqrt{\mu\varepsilon}) \quad (8)$$

where k_{cmn} is the cut-off wave number of each high order mode.

TEM mode propagating velocity which relates with the light speed $c = 1/\sqrt{\mu\varepsilon}$ in coaxial waveguide and the transmitting speed of high order modes can be expressed as the following equation [21]

$$u_{gmn} = u_p \sqrt{1 - (f_{cmn}/f)} \quad (9)$$

where $u_p = 1/\sqrt{\mu\varepsilon}$ is the phase speed of EM-wave, it is equal with the light speed c.

3 Time of flight method

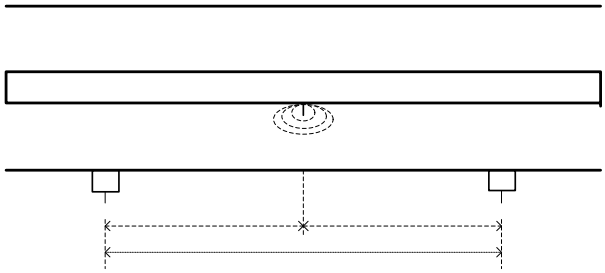

Fig.3 Time of flight PD localization system

Time of flight method is a simple and obvious way of locating PD source in GIS. As shown in Fig 3, when PD signal propagating in GIS, the time of it arriving at UHF sensors are different as the lengths of the propagation routes are different, so the time of flight technique locates the PD source by calculating the time difference between the wave fronts of PD signal arriving at two UHF sensors. The distance between PD source and UHF sensor can be calculated by the following equation [17]:

$$X_1 = \frac{X - (X_2 - X_1)}{2} = \frac{X - c_0 \cdot \Delta t}{2} \quad (10)$$

where X is the distance between two sensors, X_1 and X_2 are the relative distance between PD source and two sensors, c_0=0.3m/ns, △t is the time difference which is determined by the initial pulses of signals detected by two sensors.

Equation (10) is always used to locate PD source in time of flight method. The time of signal initial pulse is used as reference time to calculate the time difference △t. But if the initial pulse of the PD signal is small and blurry or its SNR is too low, the △t can not be easily identified and the time of flight method can hardly be applied effectively and will induce errors.

4 The Characteristics of EM-wave Propagation Route

4.1 Theory

EM-waves are emitted to the space around PD source in all directions when PD happens in GIS. The EM-wave propagates in GIS in such way that it transmits to the waveguide wall in a certain angle and reflected in the same angle. Considering that the incidence angle is related with the radial position of PD source in GIS, the EM-waves propagation routes are analyzed as PD source locating near inner conductor or outer conductor.

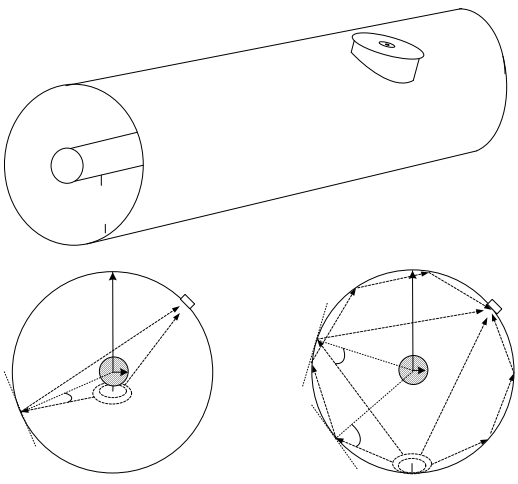

(a)PD near inner conductor (b)PD near outer conductor

Fig.4 The EM-wave propagating route of PD in different sites

When PD source locates near the inner conductor of GIS, the EM-waves propagation routes from PD source to sensor was showed in Fig 4(a). The incidence angle θ_i in the transverse section is small as the PD source is near the centre conductor. One EM-wave component arrives at the sensor in most direct path while other EM-wave components propagate to the sensor by reflecting on the waveguide wall. But the situation is different when PD source locates near the outer conductor, as shown in Fig 4(b). The incidence angles θ_i in the transverse section are different and become larger as the PD source is near the edge. While one EM-wave component transmits to sensor in direct path and another component reflected to sensor by the waveguide wall, two identical EM-wave components propagate to sensor by reflecting around the inner surface of outer conductor as θ_i is close to 90 degree.

It can be seen that the EM-wave propagation route in GIS is related with the PD source radial position and the position of sensor. Hence, the relationships between EM-wave signals and the positions of PD source and sensor were researched in the following sections.

4.2 Simulation

In order to studying the characteristic of EM-wave excited by partial discharge propagating route in GIS, the simulation model shown in Fig 5 was built and simulated by FDTD method. The inner conductor radius *a* and outer conductor radius *b* were set to 5cm and 24cm, the length of the chamber was 2m and two end ports were set as absorbing boundary. PD source was set near inner conductor (PD 1) and near outer conductor (PD 2). Three probes were set at the positions of $\varphi=0^0$, $\varphi=90^0$ and $\varphi=180^0$ on the inner surface of outer conductor with 1m distance apart from PD source respectively.

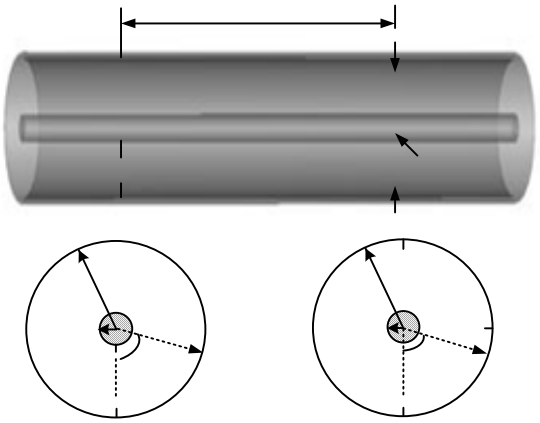

Fig.5 PD propagation route simulation model

The PD current can be approximated described by a Gaussian function as follows [18]:

$$i(t) = I_0 e^{-(t-t_0)^2/2\sigma^2} \qquad (11)$$

where I_0 is the peak value of current pulse, σ is the time attenuation constant.

In this paper, the amplitude of PD current pulse I_0 was set to 10mA, σ was set to 0.17ns and t_0 was set to 0.9ns, as shown in Fig 6. PD current flowed in the radial direction and the path length was 10mm. The electric field signals of PD1 and PD2 detected by three probes were shown in Fig 7.

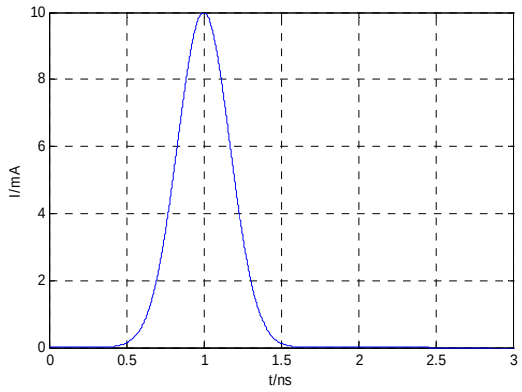

Fig.6 Partial discharge current pulse

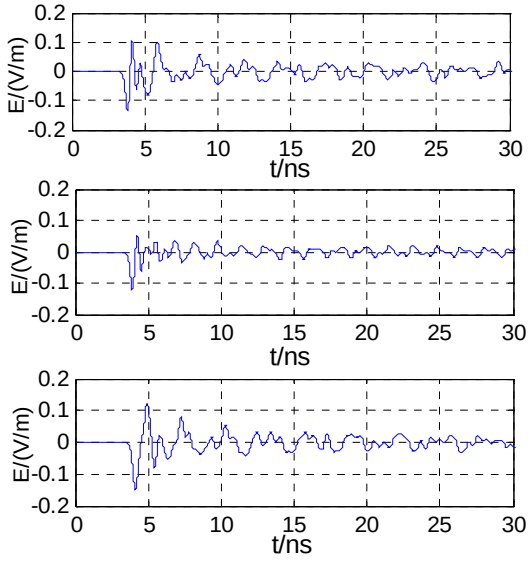

Fig.7 The electric field signals of PD 1 detected by three probes

As shown in Fig 7, the initial pulses of signals detected by probes are all big and clear. It can be explained by that the first pulse arriving at sensor is TEM mode because it propagates faster than high order modes and TEM mode is big while PD source locating nears the inner conductor. The arriving times of initial pulses are about 3.5ns and the initial time of PD pulse is about 0.2ns, the time difference is about 3.3ns with 1m distance between the two probes. Hence, the propagation rout of initial pulse was consistent with the direct path.

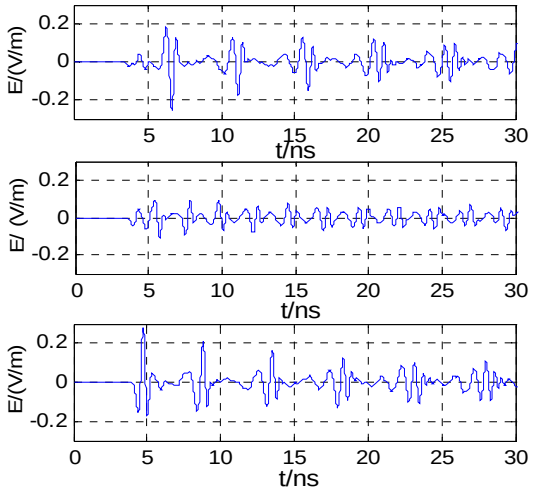

Fig.8 The electric field signals of PD 2 detected by three probes

Fig 8 shows that the signals detected by three probes are different and the initial pulses of signals are all small and hard to be identified. It means that the regular time of flight method can't be used properly. This is because that TEM mode is small as PD source locates near the outer conductor. But after several pulses there were peak pulses appeared both in the signals detected by probe 1 and probe 3 while the signal of probe 2 has not apparent peak pulse. This phenomena can be explained by that probe 1 and probe 3 located at the positions of $\varphi=0^0$ and $\varphi=180^0$, the two identical EM-wave components emitted by PD source travelling around the inner surface of the outer conductor in opposite directions and arrived at the probes synchronously by travelling the same distance and produce peak pulses while arrived at probe 2 with travelling different distance which was set at $\varphi=90^0$ position.

The first peak pulses of signals detected by probe 1 and probe 3 appear at different times which are about at 6.6ns and 4.7ns and the time difference is about -1.9ns. The distances of EM-wave travelled from PD source to two probes can be calculated as $l_1=\sqrt{(2\pi\cdot b)^2+1^2}\approx 1.81m$ and $l_3=\sqrt{(\pi\cdot b)^2+1^2}\approx 1.25m$. The time difference $\Delta t=(l_3-l_1)/c_0=-1.87ns$, and this calculation result match the simulation result well.

The analyses above indicate that the initial pulse can be discriminated clearly and the propagation route is direct path when PD source locates near the inner conductor. The initial pulse of signal is small and hard to be identified when PD source locates near the outer conductor, but peak pulses will appear in the signal when sensor locates at the position of $\varphi=0^0$ or $\varphi=180^0$ and the propagation route of peak pulse is travelling around the inner surface of outer conductor.

4.3 Experiment

4.3.1 Experiment circuit

For validating the simulation result of the characteristic of EM-wave propagation route in GIS, the PD detecting system in an actual GIS was built in laboratory as shown in Fig 9. The type of step-up transformer is 380/150kV and the voltage regulation range is 0~146kV. The high voltage output by transformer is connected to GIS high voltage conductor via current limiting reactor. There were two epoxy spacers in GIS with the distance of 1m. The radius of the inner conductor was 5cm and the inner radius of the outer conductor was 24cm. The GIS chamber was filled with 0.4MPa SF_6 gas. Three external UHF sensors were placed on one spacer with the position of $\varphi=0^0$, $\varphi=90^0$ and $\varphi=180^0$ respectively. The signals detected by external sensors were amplified by two UHF amplifiers respectively (gain 40dB) and transmitted to the digital oscilloscope (Aglient 54853A) with the maximum sampling rate of 20GS/s through 5m coaxial cable with the characteristic impendence of 50Ω.

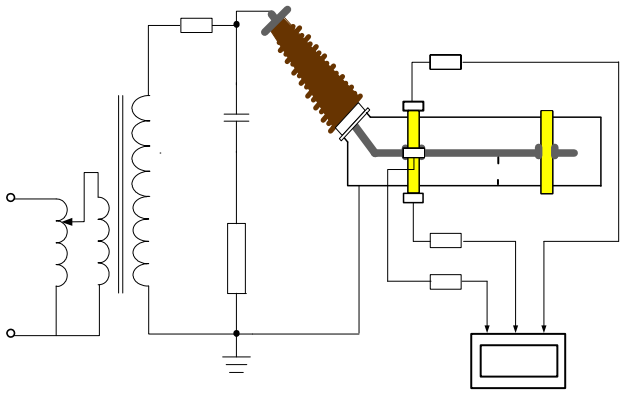

Fig.9 The circuit of PD detection in GIS

In order to making the experiment result to be more effective, the insulation defect in the actual GIS was set to be similar with simulation condition. Firstly, as shown in Fig 10(a), an artificial defect was constructed by fixing a 10mm needle with the diameter of 1mm on the inner conductor, which accorded with the condition of PD1 in the simulation model (Fig 5). Then for modelling the condition of PD2 in the simulation model, the needle was fixed on the outer conductor of the GIS, as shown in 10(b).

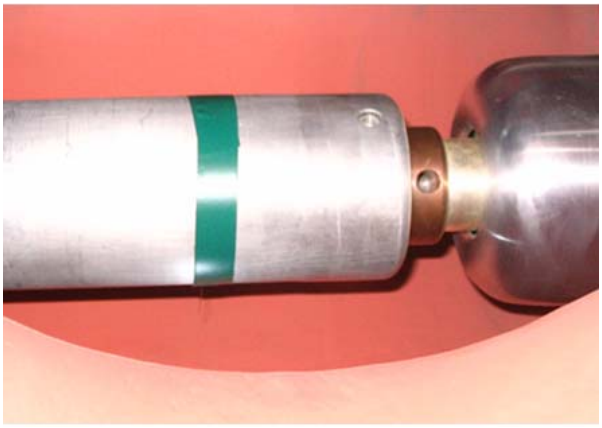

(a) needle on inner conductor

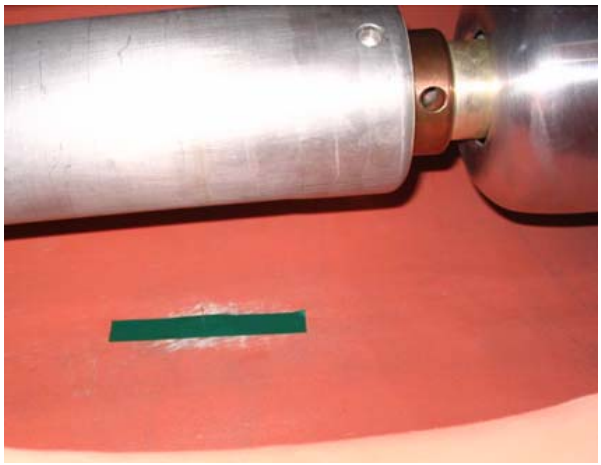

(a) needle on outer conductor

Fig.10 The insulation defect model

4.3.2 UHF sensor

In order to reduce the effect of the sensor on the detected PD signal spectrum, a broad band antenna was investigated. As one of a class of frequency-independent antennas, the spiral antenna was designed as UHF sensor for PD detection. The sensor configuration was shown in Fig 11, which bandwidth was from 500MHz to 1500MHz. The antenna pattern was etched onto copper clad polythene printed circuit board of thickness 1.6mm. The two spiral arms of the sensor are symmetrical and the impedance is about 120Ω [22]. But the measurement system has an unbalanced input impedance of 50Ω. So, an infinity balun was used for providing broadband matching for the sensor.

The artificial defect was constructed by fixing a 10mm needle with the diameter of 1mm on the inner conductor, as shown in Fig 10(a). The UHF sensor was fixed on the insulator with the positionJunhua of $\varphi=180^0$. When the voltage was step up to 45kV, the PD signal was detected. The PD signal detected with IEC60270 method was 2.6pC. The waveform and the spectrum of the signal detected by UHF sensor were shown in Fig 12.

Fig11.Planar spiral antenna

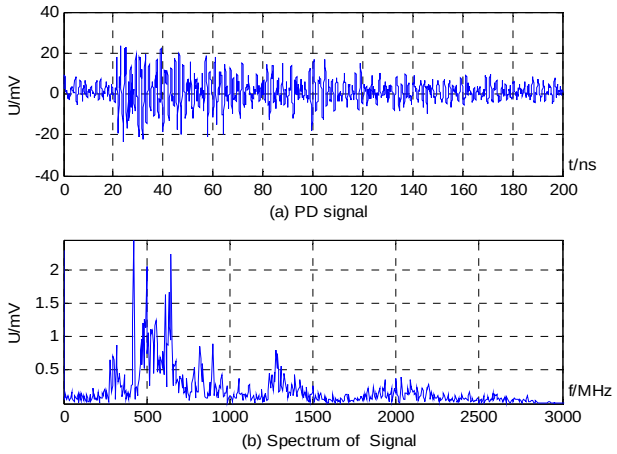

Fig12. PD signal detected by UHF sensor

Fig 12 shows that the UHF sensor can detect the PD signal sensitively. The needle defect on the inner conductor of GIS can excite PD signal with frequency excess of 2GHz. The frequencies of 400MHz~700MHz are the dominant component of the signal detected by the UHF sensor.

4.3.3 Experiment result

The PD signals detected by the three sensors were shown in Fig 13(a) when the needle was fixed on the inner conductor. It can be seen that the initial signal pulses of three sensors at different φ position are all big and clear, and the time instants of initial pulses are same. This characteristic accords with the simulation results. But the initial pulses were not as big as in simulation result, and this can be explained by that the signals were detected by external antenna. The signals period time and strength were increased as the signal reflected by the insulators and the metal lids at both ends of the chamber.

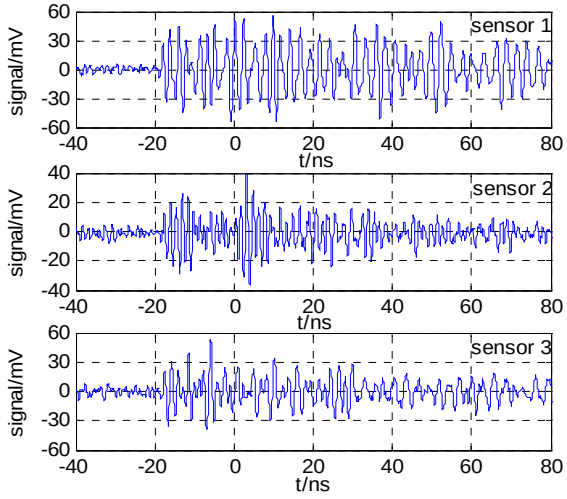

(a).PD Signals of needle on the inner conductor

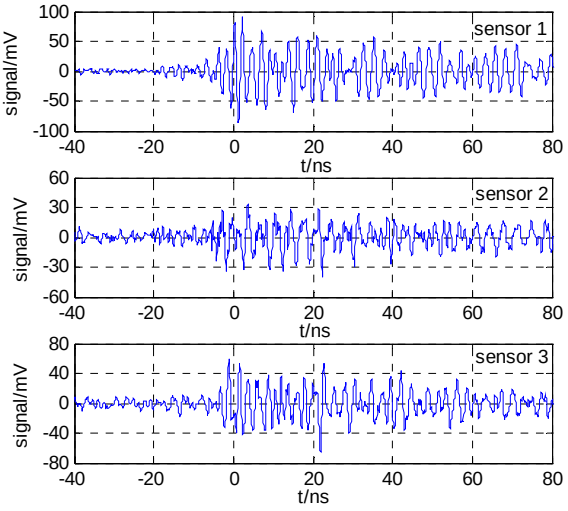

(b). PD Signals of needle on the outer conductor

Fig.13 PD Signals excited by needle in GIS

When the needle was fixed on the outer conductor of GIS, the PD signals detected were shown in Fig 13(b). None of the initial signal pulses of the sensors at different φ position is clear and can be discriminated. But there are peak pulses appeared in the signal of sensor 1 and sensor 3 which were placed at $\varphi=0^0$ and $\varphi=180^0$. All these characteristic

are in accord with the simulation results. The first peak pulse is easier to be discriminated than the other peak pulses which are affected by the reflected signal from insulator and mental lids.

5 PD Localization Method Based on EM-wave Propagation Route

5.1 PD Localization method

The initial pulse of EM-wave signal is small and hard to be discriminated when PD source locates near the outer conductor, so the regular time of flight method as shown in function (10) is hard to use to locate the PD source. But it can be seen from above analysis that there are peak pulses appearing in the signals when sensor located at the position of $\varphi=0^0$ or $\varphi=180^0$ and the time instant of the first peak pulse accord with the path of propagating around the inner surface of the outer conductor from PD source to the sensor. Therefore, the PD source can be located according to the time difference of the first peak pulses.

In the PD localization system such as shown in Fig 3, the equations of peak pulse time difference can be expressed as follows:

$$\begin{cases} \sqrt{(n\pi r)^2 + X_2^{\ 2}} - \sqrt{(n\pi r)^2 + (X_1)^2} = c_0 \cdot \Delta t \\ X_1 + X_2 = X \end{cases} \quad (12)$$

where $\begin{cases} n=1, & \Phi = 180^0 \\ n=2, & \Phi = 0^0 \end{cases}$

Solving the equations (5), then get

$$\begin{cases} X_1 = \dfrac{X}{2} + \dfrac{1}{2}\sqrt{(c_0\Delta t)^2 + \dfrac{4(n\pi r c_0 \Delta t)^2}{X^2 - (c_0\Delta t)^2}} & \Delta t < 0; \\ X_1 = \dfrac{X}{2} - \dfrac{1}{2}\sqrt{(c_0\Delta t)^2 + \dfrac{4(n\pi r c_0 \Delta t)^2}{X^2 - (c_0\Delta t)^2}} & \Delta t > 0; \end{cases} \quad (13)$$

where X is the distance between two sensors, X_1 and X_2 are the relative distance between PD source and two sensors, c_0=0.3m/ns, r is the inner radius of the outer conductor. △t is the time difference between the first peak pulses of signals detected by two sensors.

Hence, PD localization method in time domain based on the characteristics of EM-wave propagation route is proposed as follows. It is necessary to identify the PD source radial position at first for locating PD source correctly. The characteristics of EM-waves are different according with the PD source position as analysis above. The EM-wave signal at different φ position can be detected by moving the external UHF sensor. If the characteristic of EM-wave match the EM-wave characteristic of PD source locating near the outer conductor, the equation (13) can be applied to locate the PD source, else the equation (10) will be used for PD localization.

5.2 Laboratory test

To check the validity of the PD localization method in time domain based on EM-wave propagation route, the actual GIS PD locating test system was constructed as shown in Fig 14 which was based on the PD detection circuit of Fig 9 in laboratory. A needle was fixed on the outer conductor of the GIS which is 0.7m apart from the left spacer. Two external UHF sensors were used to locate the PD source.

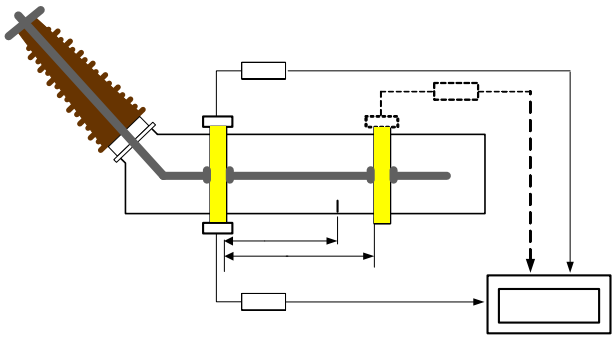

Fig.14 The PD localization system in GIS

At first, it is necessary to identify the PD source radial position. Sensor 1 and sensor 2 were place on the same spacer such as the left spacer with the interval of $\varphi=180^0$ as shown in Fig 14. The sensors were moved by keeping the interval angle unchanged and stopped when the signal amplitude became the largest. The sensors were at the positions of $\varphi=0^0$ and $\varphi=180^0$ relative to the position of PD source. The signals were shown in Fig 15.